ARCHIVES OF ELECTRICAL ENGINEERING VOL. 61(3), pp. 347-357 (2012)

DOI 10.2478/v10171-012-0028-9

Research of selected electric and magnetic properties of railway rail

KAMIL KIRAGA, ELŻBIETA SZYCHTA

Institute of Transport Systems and Electrical Engineering
Technical University of Radom
e-mail: {k.kiraga/e.szychta}@pr.radom.pl

(Received: 11.01.2012, revised: 16.03.2012)

Abstract: The article presents measurement methods serving to determine electric and magnetic properties of rails (60E1) used to construct railroad turnouts. Knowledge of a rail's electric and magnetic properties is necessary to analyse the phenomena in the rail's internal structure when under impact of a powerful electromagnetic field. The electric and magnetic properties will also help to develop a simulation model of turnout induction heating in 2D and 3D space.

Key words: rail transport, measurements of electromagnetic properties of rails

1. Introduction

Rails (stock) are fundamental design elements of a turnout, beside switch points, sliding chairs or switching closure assemblies. Rails are principally designed to set the proper travel direction of rolling stock wheel sets. Shape of a rail comprises three characteristic sections: head (the part along which rolling stock wheels move), web, and foot (the part supporting the whole and carrying the load on to sleepers) [4].

The following elements of a heating circuit are analysed as part of testing aimed at developing a method of induction turnout heating: structure of rail material, resistivity and magnetic permeability, skin effect and depth of magnetic field penetration into the rail structure, discharge of active power in the form of impact of the magnetic field on the rail. These parameters depend, inter alia, on magnetising current frequency and are not defined by rail manufacturers. It appears rails may come from different charges, may be produced by means of diverse rolling, straightening, and possibly hardening technologies. It was therefore important to determine locations from which rail samples would be removed. To generate a maximum quantity of data for further research, samples were withdrawn (cut) from key points of a rail. Sample removal locations and their geometric dimensions are shown in Figure 1.

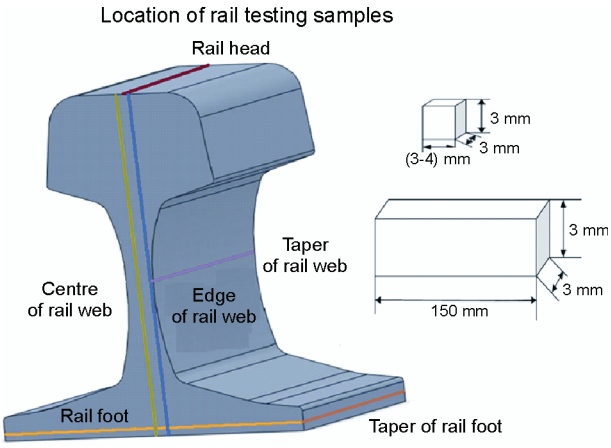

Fig. 1. 60E1 sample removal locations and their geometric dimensions

Determining key electric and magnetic parameters of construction materials for railroad turnouts was essential in designing a system of induction heating and employed a variety of testing methods.

2. Electric and magnetic properties of e160 rail

Electric and magnetic parameters were determined by means of the following methods:

- **Four-point linear probe method** to determine electric resistivity (taken into consideration as rotary currents arise when the magnetic field penetrates the internal structure of a rail) [2, 5, 6].

A flow diagram of electric resistivity measurements is illustrated in Figure 2.

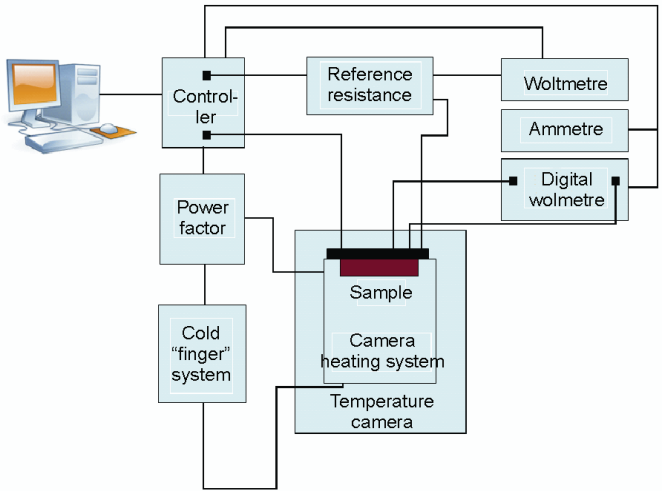

Fig. 2. Flow diagram of electric resistivity measurement system

Electric resistivity can be measured by means of a four-point linear probe and a measurement system which employs a PC to record the voltage drop across a tested sample and across a reference resistor R_w. Voltage is checked by running the current (10 times) in two directions. Once averaged, both the results are added and contact effects are eliminated in this way. The result is averaged and saved to the memory. The current's value can be calculated according to:

$$I_x = \frac{U_{Rw}}{R_w}, \tag{1}$$

where: I_x – measurement current [A], U_{Rw} – voltage drop across the reference resistor [V], R_w – reference resistor [Ω].

With known geometric dimensions of the sample, that is, its a height and width b, electric resistivity can be determined on the basis of:

$$\rho = \frac{U_x}{I_x} \cdot \frac{S}{l} = R \cdot \frac{S}{l}, \tag{2}$$

where: ρ – electric resistivity [Ωm], U_x – voltage drop across the sample [V], I_x – measurement current [A], S – cross-section surface of the sample [m^2], l – distance between the measurement probes [m].

Table 1 summarises results of electric resistivity measurements for samples from characteristic rail locations

Table 1. Values of electric resistivity for the tested samples

Source of the sample	Mean electric resistivity ρ [Ω m]
Edge of rail web	$2.62 \cdot 10^{-7}$
Centre of rail web	$2.85 \cdot 10^{-7}$
Rail foot	$2.75 \cdot 10^{-7}$
Taper of rail foot	$2.57 \cdot 10^{-7}$
Taper of rail web	$2.7 \cdot 10^{-7}$
Rail head	$2.58 \cdot 10^{-7}$

- **HP BRIDGE**: active and passive magnetic hardness as well as the loss tangent are determined. Initial magnetic hardness can also be defined since the intensity of the magnetic field is low.

Hewlett Packard 4284 A 20 Hz-1 MHz Precision LCR Meter helps to conduct measurements in order to determine relative magnetic permeability μ of selected rail sections.

A connection link is replaced with a measurement coil of known length l and number of coils z. A sample is placed inside the coil. The bridge circuit is supplied with AC. A millivoltmetre of very high internal resistance is connected in parallel to the coils with the sample inside. It can measure the voltage drop across this element and, consequently, select the magnetising field as appropriate. The device also provides for de-magnetising of samples using

a 50 Hz field whose amplitude reduces towards zero, for regulation and stabilisation of temperature.

The system used to determine relative magnetic permeability μ of the tested rail sections consisted of: a PC and its software, Aligent 34401 A 6 ½ Digital Multimeter, (hp) Hewlett Packard 4284 A 20 Hz – 1 MHz Precision LCR Meter, and a measurement coil.

Figure 3 contains a diagram of the measurement stand serving to determine μ.

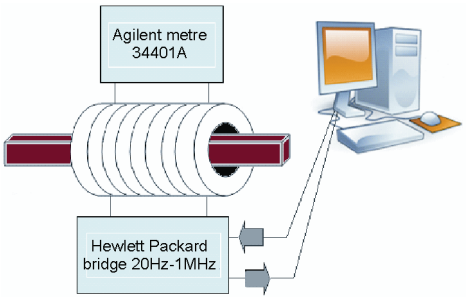

Fig. 3. Measurement apparatus serving to determine relative magnetic permeability μ

An AC bridge is the chief component of the system which provides for accurate measurement of combined magnetic permeability:

$$\underline{\mu} = \mu_{\mathrm{cz}} + \mu_{\mathrm{b}}. \tag{3}$$

The combined permeability comprises:

- the component active magnetic permeability μ_{cz} responsible for magnetising processes,
- the component passive magnetic permeability μ_{b} responsible for magnetic losses.

The active magnetic permeability can be formulated [2, 3]:

$$\mu_{\mathrm{cz}} = \frac{(L_{\mathrm{x}} - L_0)\cdot l}{\mu_0 z^2 S_{\mathrm{p}}} + 1, \tag{4}$$

where: L_{x} – inductivity of the coil containing the sample [H], L_0 – inductivity of an empty coil [H], μ_0 – magnetic permeability of the vacuum $\mu_0 = 4\pi\cdot 10^{-7}$ H/m, S_p – cross-sectional surface area of the tested sample [m^2], z – number of coils, l – length of the coil [m].

As $\mu_{\mathrm{cz}} \gg 1$, 1 is ignored in the calculations. The passive magnetic permeability is computed [2]:

$$\mu_{\mathrm{b}} = \frac{R_{\mathrm{rdz}}\cdot l}{\mu_0 z^2 \cdot 2\pi \cdot f \cdot S_p}, \tag{5}$$

R_{rdz}, or the core's resistance, is calculated:

$$R_{rdz} = R - R_0, \tag{6}$$

where: R_0 – resistance of an empty coil [Ω], R – resistance of the coil containing the sample [Ω].

Substituting (6) to (5) produces the following equation of passive magnetic permeability [3]:

$$\mu_{\mathrm{b}}=\frac{R_{\mathrm{rdz}}\cdot l}{\mu_0 z^2 2\pi f S_p}=\frac{(R-R_0)\cdot l}{\mu_0 z^2 2\pi f S_p}. \tag{7}$$

Measuring voltage drop across the resistance R helps to determine intensity of the electric current across the winding and then the intensity of the magnetic field at which magnetic permeability is measured using the dependence:

$$H=\frac{z\cdot U}{l\cdot R}, \tag{8}$$

where: z – number of coils, U – voltage drop across the resistor R [V], l – length of the measurement coil [m].

Figure 4 illustrates the initial magnetic permeability $\mu_{\mathrm{initial}}=f(f)$ of a sample from the rail web edge (red) and $\mu_{\mathrm{initial}}=f(f)$ of a sample from the rail's head (black) as well from the rail's core (the green curve).

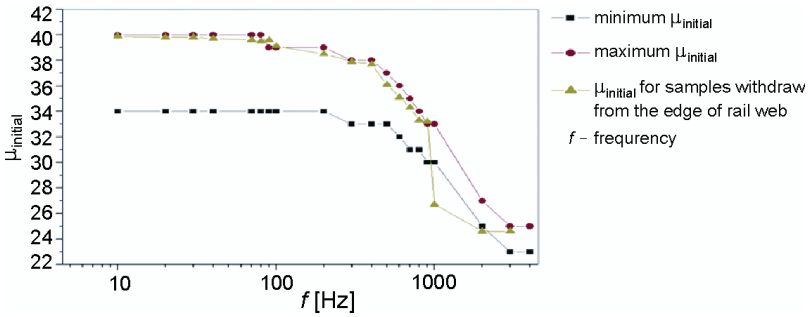

Fig. 4. Magnetic permeability $\mu_{\mathrm{inital}}=f(f)$ for a sample from the edge of rail web and $\mu_{\mathrm{inital}}=f\ (f)$ for the remaining samples

- **A FLUXMETRE** serves to plot the curves $B=f(H)$ and $\mu=f(H)$,

Prime magnetising curves were determined by means of the measurement system shown in Figure 5.

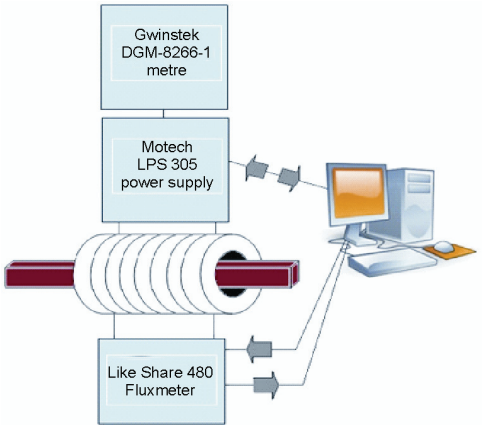

Fig. 5. Measurement system employing the fluxmetre and its components

The tested sample is placed inside the coil in magnetising and measurement winding. A fluxmetre to measure magnetic flow variations in the tested material sample is the element of the measurement system. Variations in the tested material sample result from commutations of the current across the magnetising winding z_m. The electric current pulse induced in the measurement winding over time dt is measured by the fluxmetre. The magnetic flow variations $d\Phi$ generate an electromotor force ε which can be expressed:

$$\varepsilon = -\frac{d\phi_c}{dt} = -z_p \cdot \frac{d\phi}{dt}, \tag{9}$$

Fluxmetre readings are proportional to magnetic flow variations. When a uniform external magnetic field is applied, magnetic induction B can be computed according to:

$$B = \frac{d\phi}{2z_p S}, \tag{10}$$

where: S is the cross-sectional surface area of the tested sample.

The sample is demagnetised prior to each measurement by means of the system.

A prime magnetising curve for a sample from the rail web and maximum magnetic permeability in respect of the same sample determined using the fluxmetre are shown in Figure 6.

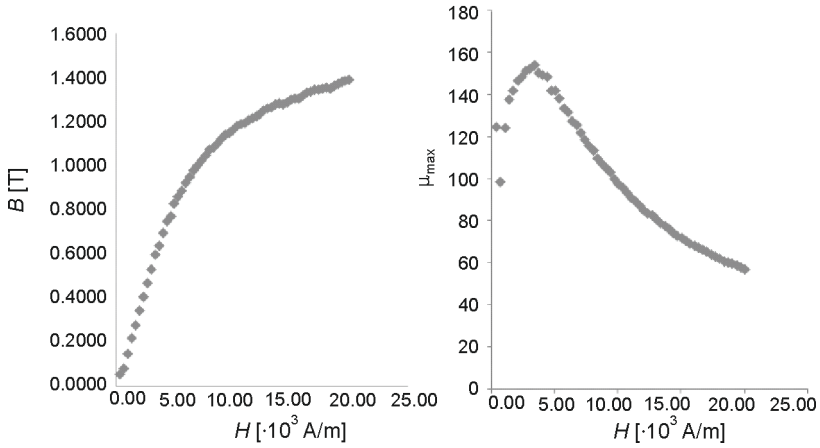

Fig. 6. Curves $B = f(H)$ and $\mu = f(H)$ for a sample of the rail web

- **COERCION METRE** measures intensity of the coercion field.

Intensity of the coercion field of magnetically soft and hard materials can be measured by means of a coercion metre. The relevant measurement diagram is presented in Figure 7.

Magnetic coercion (also referred to as coercive force) is the value of an external magnetic field that must be applied to a material (e.g. a ferromagnetic material) to bring the magnetic residue down to zero. The magnetic residue (also remanence or residual magnetisation) is the magnetic induction remaining after an external magnetic field magnetising a given material is removed.

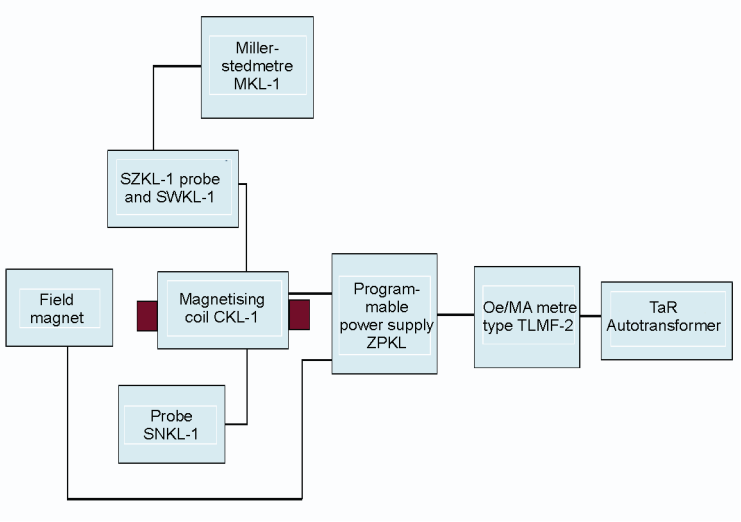

Fig. 7. Measurement diagram using a coercion metre and its components

Table 2 summarises measurement results of magnetic coercion intensity for samples removed from key rail locations.

Table 2. Coercion field intensity in respect of all samples

Source of the sample	H_c [A/m]
Edge of rail web	823
Centre of rail web	774
Rail foot	778
Taper of rail foot	912
Taper of rail web	830
Rail head	850

- **PPMS VSM** was utilised to plot the curve $J = f(H)$,

A Physical Property Measurement System (PPMS) by Quantum Design (San Diego, USA) is a unique, state-of-the-art concept of a laboratory facility.

The PPMS platform comprises the following elements:

- superconducting magnet of up to 7 Tesla (and, more recently, even 16 Tesla),
- specific heat measurement system (Heat Capacity 4He) in the temperature range 2 K-400 K and magnetic fields of up to 7 Tesla,
- specific heat measurement system (Helium-3) in the temperature range 350 mK-350 K and magnetic fields of up to 7 Tesla,
- AC/DC magnetisation measurement system for magnetic fields of up to 7 Tesla,
- vibration magnetometer VSM for precise magnetising measurements In a broad temperature range of 2 K to 1000 K. It is additionally fitted with an oven (P527 Sample Magnetometer Oven) for measurements of up to 1000 K.

- heat conductivity and thermal force measurement system,
- measurement capability of electric resistance in the range of 350 mK,
- vertical rotator to regulate sample position in relation to the magnetic field,
- and an easyLab Pcell 30 kbar pressure chamber to measure resistance at high pressure of up to 30 kbar.

A magnetometer suction cup with the vibrating sample was employed to plot prime magnetising curves and to determine saturation of the tested rail samples [1-3].

A sample is positioned on a non-magnetic, mobile bar and vibrates vertically at a set frequency. The sample's oscillations generate (induce) a variable voltage signal in the measurement coil system under impact of the magnetic field. The signal is proportional to the magnetic moment of the sample and to parameters characterising its motion, i.e. to the amplitude and vibration frequency. It can be described as follows:

$$V_{cewki} = -\left(\frac{d\phi}{dz}\right)\left(\frac{dz}{dt}\right) = CmA\omega\sin(\omega t), \tag{11}$$

where: C – proportionality constant, m – a known moment of the sample, A – vibration (oscillation) amplitude, ω – frequency.

A flow diagram of vibrating sample magnetometer (VSM) is illustrated in Figure 8.

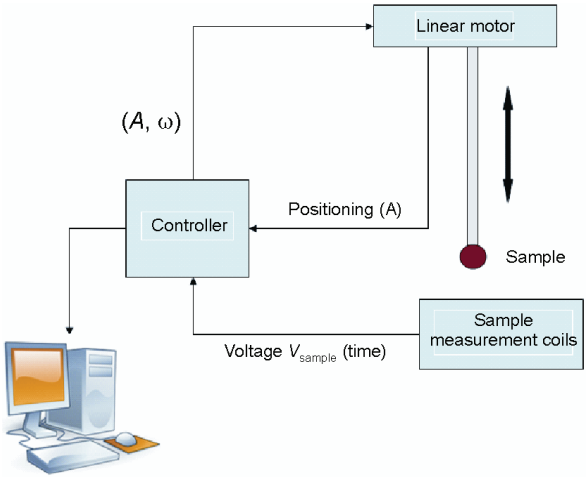

Fig. 8. Flow diagram of VSM measurement platform

Figure 9 presents a magnetising curve $J = f(H)$ and magnetic saturation J_s for rail head samples.

- **ACMS** determines combined magnetic susceptibility, including its real and imaginary components, the loss tangent for varied intensities of the magnetic field and for different temperatures.

ACMS (AC Measurement System) provides for a single sequence of measurements of AC and DC susceptibility in a broad temperature range from 1.9 K-350 K. AC measurements are

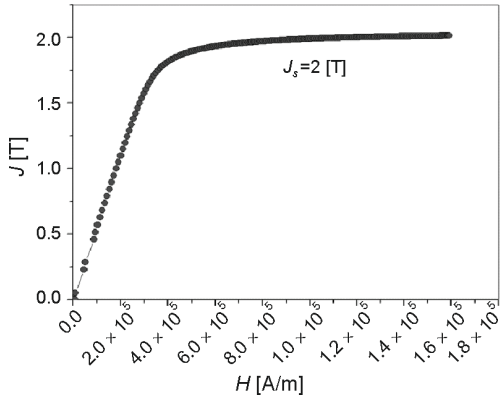

Fig. 9. Magnetising curve $J = f(H)$ and magnetic saturation J_s for rail head samples

thrice as sensitive (2×10^{-8}emu (2×10^{-11} Am^2) at 10 kHz) as DC measurements. Better results may be occasionally obtained by means of the DC method. Application of a powerful external field can increase the sample's magnetic moment and generate signals above the noise (the range of DC magnetising DC: 2.5×10^{-8} Am^2-5×10^{-3}Am^2 (2.5×10^{-5}emu-5emu). DC measurement uses a constant field in the measurement area where the sample moves by means of detection coils and induces voltage there according to Faraday's law. Amplitude of this signal depends on the sample's magnetic moment and the rate of its removal. As part of this system, the sample is extracted at an approximate speed of 100 cm/s. The signal's force grows considerably as a result compared to other systems. The measurements can be executed as a function of both temperature and of the magnetic field.

Flow diagram of ACMS and its key elements are shown in Figure 10.

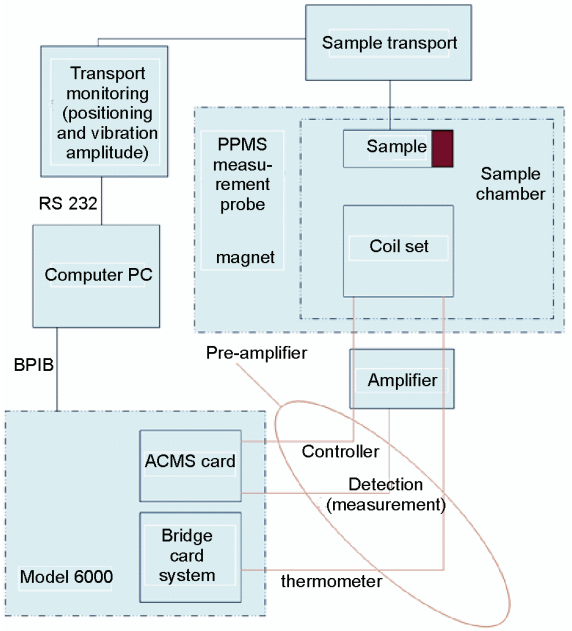

Fig. 10. Flow diagram of ACMS

Table 3 summarises loss factors on eddy currents and magnetic hysteresis for samples collected in key rail locations determined at varied temperatures by means of ACMS platform.

Table 3. Loss factors on eddy currents and magnetic hysteresis

Source of the sample	Temperature [°C]	Loss factor on eddy currents w [10^{-4} s]	Loss factor on magnetic hysteresis loop [10^{-5} m/A]
Edge of rail web	0 [ºC]	2.49	2.31
	25 [ºC]	2.33	2.62
	–25 [ºC]	2.7	2.44
Centre of rail web	0 [ºC]	2.53	2.42
	25 [ºC]	2.33	2.8
	–25 [ºC]	2.72	2.78
Rail foot	0 [ºC]	2.31	1.42
	25 [ºC]	2.13	1.45
	–25 [ºC]	2.49	1.63
Taper of rail foot	0 [ºC]	2.39	1.94
	25 [ºC]	2.2	1.97
	–25 [ºC]	2.6	1.77
Taper of rail web	0 [ºC]	1.83	1.55
	25 [ºC]	1.69	1.76
	–25 [ºC]	2.56	1.83
Rail head	0 [ºC]	2.62	2.49
	25 [ºC]	2.42	2.4
	–25 [ºC]	2.83	2.68

3. Summary of measurement results

Sensitivity of the magnetometer used in the research (Physical Property Measurement System Quantum Design) was 10^{-7} emu. This range was sufficient and allowed the examination of the process of magnetization of samples taken from the railway rail. The uncertainty of temperature measurement is ± 0.2 K. The uncertainty of the magnetic field of ± 1%. Superconducting magnet (7 T) is the uncertainty of the order of 1% for field –7 T to 7 T. Absolute errors of physical quantities measured by other measuring methods presented in this article did not exceed 7%.

4. Conclusions

Induction heating can be applied to heating of rail turnouts by employing enhanced-frequency eddy currents as basic energy carriers. To this end, as much information regarding

rail properties as possible must be collected (since rails are among chief design elements of a turnout and heating wires will be placed on top of them). The rail's internal structure, its resistivity, and magnetic permeability must therefore be analysed as the rail will receive the magnetic field's energy.

The measurement methods discussed in this article helped to determine electric and magnetic properties of 60E1 rail, a component of turnouts for high-speed trains. Values of factors introduced in this article will be employed in the authors' continuing research in two ways:

- They will contribute to a simulation model of turnout induction heating in order to follow behaviour of rails across which eddy currents flow and to observe the associated electromagnetic effects.
- An actual system of turnout heating will be constructed on the basis of the simulation test results.

The results presented in this paper are the authors' unique contribution to the process of developing a turnout induction heating system.

References

[1] Binns K.J., Lawrenson P.J., Trowbridge C.W., *The Analytical and Numercial Solution of Electric and Magnetic Fields*, A Wiley-Interscience Publication, John Wiley & Sons, INC., New York (1995).
[2] Gignoux D., Schlenker M., *Magnetism Fundamentals*, Springer, Grenoble, France (2005).
[3] Jiles D., *Introduction to Magnetism and Magnetic Materials*. Chapman & Hall, New York (1991), ISBN 0-412-386-30-5.
[4] Kiraga K., Szychta E., Andrulonis J., *Wybrane metody ogrzewania rozjazdów kolejowych – artykuł przeglądowy. (Chosen methods heating crossover railway system – inspecton article).* Przegląd Elektrotechniczny 86(2) (2010), (in Polish).
[5] Michalik J., Buday J., *Electric Machines.* EDIS – University of Žilina, Žilina (2006).
[6] Sikora R., *Teoria pola elektromagnetycznego.* (*Electromagnetic Field Theory*). Wydawnictwo Naukowo-Techniczne, Warszawa (1997), (in Polish).